IEEE Access
Multidisciplinary : Rapid Review : Open Access Journal

Received 7 February 2023, accepted 2 March 2023, date of publication 6 March 2023, date of current version 10 March 2023.

Digital Object Identifier 10.1109/ACCESS.2023.3253201

RESEARCH ARTICLE

Transmission Expansion Planning Considering a High Share of Wind Power to Maximize Available Transfer Capability

AHMAD M. ALSHAMRANI[1], **MOHAMMED A. EL-MELIGY**[2], **MOHAMED ABDEL FATTAH SHARAF**[3], **WIGDAN AREF MOHAMMED SAIF**[3], **AND EMAD MAHROUS AWWAD**[4]

[1]Statistics and Operations Research Department, College of Science, King Saud University, Riyadh 11451, Saudi Arabia
[2]Advanced Manufacturing Institute, King Saud University, Riyadh 11421, Saudi Arabia
[3]Industrial Engineering Department, College of Engineering, King Saud University, Riyadh 11421, Saudi Arabia
[4]Electrical Engineering Department, College of Engineering, King Saud University, Riyadh 11421, Saudi Arabia

Corresponding author: Mohamed Abdel Fattah Sharaf (mfsharaf@ksu.edu.sa)

This work was supported by the Deputyship for Research and Innovation, Ministry of Education, King Saud University, under Project IFKSURG-2-1322.

ABSTRACT To have an effective transmission network and support free trading, the open and non-discriminatory access to transmission services for all market participants under all conditions is of significant concern. To this end, a sufficient value of available transfer capability (ATC) is required, which can significantly affect the electricity market efficiency. This paper constructs a methodology for reinforcing an existing transmission network considering wind power investment to enhance ATC. In this regard, a bi-level structure is adopted whose upper level is the joint transmission expansion planning (TEP) and wind power investment subject to the technical power grid limitations. After solving the upper level, a security-constrained economic dispatch (SC-ED) is formulated to acquire the optimal generation scheduling. Then, the lower level is designed to calculate the ATC. To solve this problem, the SC-ED is first replaced by its primal and dual feasibility constraints and strong duality equality. Then, these constraints are added to the upper level. The lower level is also replaced by its corresponding constraints. Consequently, a bilinear single-level optimization problem is extracted, which is further solved by employing Konno's cutting plane algorithm. The experimental results on the IEEE 24-bus RTS show the proposed method's effectiveness. It is indicated that the ATC can be improved by 27.2 % using the formulated model at the expense of more investment cost resulting in less load shedding and less wind curtailment.

INDEX TERMS Available transfer capability, bi-level optimization, bilinear programming, Konno's algorithm, transmission expansion planning, wind power investment.

NOMENCLATURE

A. INDICES AND SETS

Ω^N	Set of buses indexed by i, j.
Ω^S	Set of scenarios indexed by s.
$\Omega^{DV} = \Omega^{DV_1} \cup \Omega^{DV_2}$	Set of decision variables of the bilinear problem divided into two different sets Ω^{DV_1} and Ω^{DV_2}.
Ω_N^{RA}, Ω_N^{SA}	Set of buses in receiving (sink) and sending (source) areas.

The associate editor coordinating the review of this manuscript and approving it for publication was Ehab Elsayed Elattar.

B. PARAMETERS

b_{ij}	Susceptance of lines.
c_i^T	Production cost of a thermal unit.
C_i^W, C_{ij}^L	Annualized investment cost of a wind farm and a transmission line.
M_1	Big-M parameter.
P_{is}^{D0}	Electric demand.

$\overline{P}_{ij}^{L}$	Capacity of a line.
$\overline{P}_{i}^{T}$	Capacity of a thermal unit.
K_i^D, K_i^T, K_i^W	Change rate in load and generation (thermal and wind) as λ_s increases.
N_s	Number of hours in scenario s.
$\underline{\delta}_i, \overline{\delta}_i$	Minimum and maximum voltage angle.
π_{is}	Capacity factor of a wind farm ($0 \leq \pi_{is} \leq 1$).
ω	Weighting coefficient.

C. VARIABLES

$P_{ijs}^{L}, \tilde{P}_{ijs}^{L}, P_{ijs}^{L0}$	Power flow through lines in the main problem, ATC evaluation problem and SC-ED problem.
OF_s^{lo}, OF^{up}	Lower and upper objective functions.
λ_s	A variable indicating the growth in load or generation.
$\tilde{P}_{is}^{D}$	Electric demand in the ATC evaluation problem.
$P_{is}^{T}, \tilde{P}_{is}^{T}, P_{is}^{T0}$	Power output of thermal units in the main problem, ATC evaluation problem and SC-ED problem.
$P_{is}^{W}, \tilde{P}_{is}^{W}, P_{is}^{W0}$	Power output of a wind farm in the main problem, ATC evaluation problem and SC-ED problem.
$\overline{P}_{i}^{W}$	Capacity of a wind farm.
u_{ij}^{L}	Binary variable indicating the installation status of a transmission line.
$\delta_{is}, \tilde{\delta}_{is}, \delta_{is}^{0}$	Voltage angle in the main problem, ATC evaluation problem and SC-ED problem.
$\delta_{ref,s}$	Voltage angle at the reference bus.
$\eta_{is}^{B}, \eta_{ijs}^{LP}, \underline{\eta}_{is}^{T}, \overline{\eta}_{is}^{T}$, $\underline{\eta}_{is}^{W}, \overline{\eta}_{is}^{W}, \eta_{ijs}^{L}$ & $\underline{\eta}_{is}^{\delta}, \overline{\eta}_{is}^{\delta}, \eta_{ref,s}^{\delta}$, $\eta_{is}^{KT}, \eta_{is}^{KW}, \eta_{is}^{KD}$	Dual variables associated with ATC evaluation problem.
$\eta_{is}^{B0}, \eta_{ijs}^{LP0}, \underline{\eta}_{is}^{T0}, \overline{\eta}_{is}^{T0}$, $\underline{\eta}_{is}^{W0}, \overline{\eta}_{is}^{W0}, \eta_{ijs}^{L0}$, $\overline{\eta}_{is}^{\delta 0}, \eta_{ref,s}^{\delta 0}, \underline{\eta}_{is}^{\delta 0}$	Dual variables associated with SC-ED problem.

I. INTRODUCTION

A. BACKGROUND, MOTIVATION, AND CONTRIBUTION

To facilitate the transaction amongst market participants, there must be sufficient capacity in the transmission grid to meet the increasing demand reliably and economically. Hence, expanding and reinforcing an existing transmission network considering renewable and non-renewable energy sources is necessary. Without sufficient transmission capacity, the operator must curtail a portion of electricity demand or generated wind power leading to a significant reduction in social welfare. The transmission expansion planning (TEP) problem seeks to determine the optimal location of new transmission lines for a specified planning target so that the electric load is securely satisfied. When planning for transmission investment, the system operator must ensure an adequate amount of ATC because the ATC could significantly influence the market efficiency due to its effect on the competition and reliability level of a power system. A sufficient available transfer capability (ATC) is needed in a power system to ensure that all the market players have open and non-discriminatory access to the transmission network. Hence, it is imperative to boost ATC, which will bring more benefits for suppliers and consumers by providing less congestion and enhanced power system security.

Many methodologies in the literature address the TEP problem. However, none of these approaches consider ATC enhancement a critical criterion in their planning models, showing a knowledge gap in this field. This research study aims to fill this gap by constructing a novel strategy for transmission expansion and wind power investment planning to enhance ATC. Therefore, the transfer capability between two zones can be increased, which facilitates the generation of cheaper generators such as wind energy and reduces wind curtailment. In this context, a stochastic bi-level model is introduced for the investment problem considering ATC. First, at the upper level, an investment planning model is formulated. This upper-level problem minimizes the investment and generation cost while maximizing the ATC subject to the system constraints. After obtaining the least-cost expansion plan, a security-constrained economic dispatch (SC-ED) is solved to find the optimal generation scheduling. The output results of the upper level (i.e., the optimal expansion plan of the transmission lines and wind farms) and the SC-ED problem (i.e., the optimal generation dispatch for the base case) are used in the lower level as constant parameters. The lower level is dedicated to calculating the ATC, given these parameters as input. Afterward, the computed ATC is used at the upper level to obtain the best feasible expansion plan. A schematic diagram of the proposed methodology is presented in Fig. 1, illustrating the whole procedure of the problem. The method put forth in this study is the first of its kind and has not already been presented.

To solve this problem, first, it is necessary to replace the SC-ED with its primal and dual constraints and strong duality, given the investment plan of expanding the transmission grid and wind power plants. Then, these constraints are added to the upper level, which will not change the feasible space. In addition, the lower level is also replaced by the corresponding constraints using the same method as in the SC-ED problem. As a result, a bilinear single-level optimization problem is created, which is further solved by employing Konno's cutting plane algorithm. The implementation of the

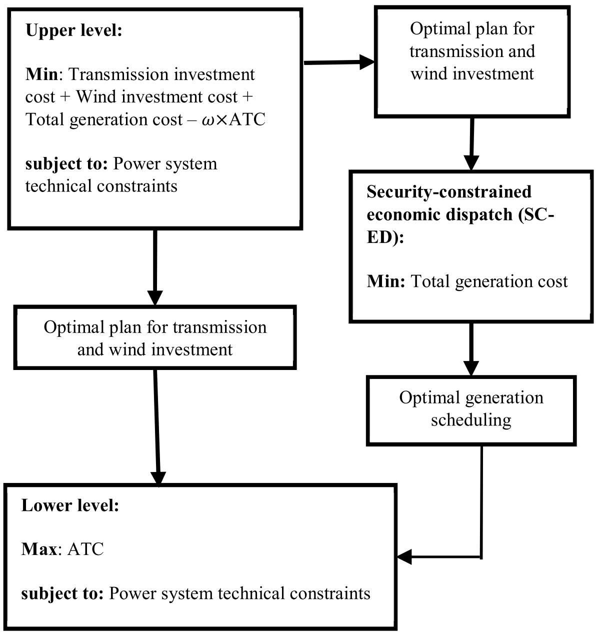

FIGURE 1. The conceptual structure of the proposed strategy for joint transmission and wind investment to enhance ATC.

proposed methodology on IEEE 24-bus RTS indicates its effectiveness in improving the ATC. Results show that more electric power from the source area can be transferred to the sink area. Furthermore, in contingencies or load growth, the amount of load shedding in the proposed model is less than that in the conventional models because more power can be transferred.

B. LITERATURE REVIEW

Transmission expansion planning is a well-known optimization problem in the field of power system planning which has been widely studied. With a high penetration level of wind power and the targets set by governments to integrate more wind energy, the transmission planning problem must be coordinated with wind power investment.

The presented models in the literature comprehensively study the transmission capacity and wind power investment problem covering different methodologies. A conic programming approach for transmission, generation, and reactive power sources planning considering a high level of wind power integration is constructed in [1]. Due to the presence of deep uncertainties in the problem, a TEP model is developed by [2] to reduce wind curtailment considering the risk factor. To assess the effect of wind farms on the TEP problem, a novel strategy is set out in [3] using scenario-based programming. Ref. [4] presents a new framework to generate representative wind and demand scenarios for the transmission investment problem considering spatial interdependencies. A co-optimization investment model for expanding transmission grid and energy storage systems (ESS) is proposed in [5]. It is shown that ESS is an efficient tool for managing transmission congestion in the presence of wind energy. A bi-level transmission grid and wind power planning model is suggested in [6] and [7]. The upper level is the wind farm and transmission network investment, while the lower level aims to clear the market. Ref. [8] presents a scheme for co-optimizing transmission expansion planning and ESS optimal sizing from a reliability viewpoint, considering the N-1 security constraints. A robust optimization model for the simultaneous investment of the transmission grid and renewable energy sources (RESs) under contingency is formulated in [9]. A joint bi-level optimization problem for transmission and wind energy investment is put forth [10]. This bi-level is further formulated as a mathematical program with equilibrium constraints seeking to minimize consumer payments. A multi-stage stochastic planning model considering a massive integration of wind power is set out in [11], in which the investment cost and reliability are used as two different objectives. A novel framework is formulated in [12] to co-optimize wind power and transmission capacity using a multi-objective optimization problem. A bi-level programming approach for scenario driven-investment model for integrated power and gas network is formulated in [13], considering wind power, power-to-gas units, and ESSs. An integrated framework for TEP and coal-fired power plants flexibility retrofits is suggested by [14] to integrate a high share of wind energy. A probabilistic transmission investment method to accommodate wind power is devised in [15] considering N-1 contingency, where Benders decomposition (BD) is employed to solve the problem. A robust optimization model for a game-based investment model for integrated electricity-gas energy systems considering a high share of wind power is presented in [16]. Transmission capacity reinforcement is studied in [17] considering the correlation, where RESs are heavily integrated into the power grid. A transmission expansion model is proposed in [18] and [19] under N-1 contingency, where the operator aims to decrease the wind power curtailment. A Monte-Carlo simulation method is employed in [20] to deal with the intermittency of wind in the planning problem using nature-inspired methods to find the optimal solution. Since including many scenarios will greatly increase the computational complexity, an approach to effectively include too many scenarios in the planning studies is proposed [21]. An AC-based transmission expansion planning is presented in [22] under uncertainty, where an evolutionary algorithm is employed to acquire the solutions. A robust optimization-based TEP with a high share of RESs is constructed in [23], where BD is used to decrease the computational burden. It is of note that the output results of the TEP problem can affect the boundary of up to congestion bidding strategy in a nodal electricity market [24]. A scenario-driven transmission and generation planning scheme is formulated in [25] to enhance the hosting capacity, where two different algorithms, including the weighted mean of vectors optimization and sine-cosine methods, are used to solve the model. Ref. [26] constructs a distributionally robust planning model considering load and wind stochastic behavior, while modeling demand response and solar power plants. A solution method to address the robust transmission planning is suggested in [27], where neither binary variables nor bilinear terms are used. Some spatial and temporal simplifications is applied to the planning problem of the generation and transmission in [28]. Authors in [29] develops an investment planning framework that finds a mix of transmission-level non-generation flexible assets: ESS, thyristor-controlled series compensators (TCSC), and transmission lines.

Motivated by the aforementioned discussion, the contribution of this work can be summarized as follows:

1) Constructing a novel strategy for transmission and wind investment planning to enhance ATC using a stochastic bi-level model.
2) Introducing a novel solution technique by replacing SC-ED problem by its primal-dual formulation and adding it to the upper level.

The remainder of the paper is organized as follows. Section II presents the mathematical model of the joint transmission and wind investment model considering ATC. Section III illustrates the solution method using the primal-dual formulation and Konno's cutting plane algorithm. A numerical experiment is presented in Section IV. Finally, section V concludes the paper with several remarks.

II. STOCHASTIC JOINT OPTIMIZATION FOR TRANSMISSION EXPANSION AND WIND INVESTMENT PLANNING CONSIDERING ATC

This section is outlined as follows. In subsection-A, the mathematical method to calculate ATC is formulated. In subsection-B, the stochastic joint investment model is constructed based on a bi-level formulation.

A. AVAILABLE TRANSFER CAPABILITY ASSESSMENT

A sufficient amount of ATC is necessary to ensure that the power grid can operate reliably over all conditions and support free trading. The ATC is an index to measure the transfer capability remaining in the transmission grid for further utilization over the existing transmission commitment [19]. To support a large number of transactions and to maintain power system stability, it is of utmost concern to precisely evaluate ATC in a network. By ignoring the transmission reliability and capacity benefit margin, the ATC can be mathematically calculated as ATC = TTC - ETC, in which TTC is the total transfer capability and the ETC is the existing transmission commitment. An optimal power flow-based model is utilized here to compute ATC, where line thermal limits are considered. The mathematical formulation to identify TTC employing a DC power flow is as follows [30] and [31]:

$$\underbrace{Maximize}_{\{\tilde{P}^T_{is},\tilde{P}^L_{ijs},\tilde{P}^W_{is},\tilde{\delta}_{is},\lambda_s,\tilde{P}^D_{is}\}} \quad OF^{lo}_s = \lambda_s \tag{1}$$

subject to :

$$\tilde{P}^T_{is} + \tilde{P}^W_{is} - \sum_j \tilde{P}^L_{ijs} = \tilde{P}^D_{is} \quad < \eta^B_{is} > \tag{2}$$

$$\tilde{P}^L_{ijs} = -u^L_{ij} b_{ij} \left(\tilde{\delta}_{is} - \tilde{\delta}_{js}\right) \quad < \eta^{LP}_{ijs} > \tag{3}$$

$$0 \le \tilde{P}^T_{is} \le \overline{P}^T_i \quad < \underline{\eta}^T_{is}, \overline{\eta}^T_{is} > \tag{4}$$

$$0 \le \tilde{P}^W_{is} \le \pi_{is}\overline{P}^W_i \quad < \underline{\eta}^W_{is}, \overline{\eta}^W_{is} > \tag{5}$$

$$\tilde{P}^L_{ijs} \le \overline{P}^L_{ij} \quad < \eta^L_{ijs} > \tag{6}$$

$$\underline{\delta}_i \le \tilde{\delta}_{is} \le \overline{\delta}_i \quad < \underline{\eta}^\delta_{is}, \overline{\eta}^\delta_{is} > \tag{7}$$

$$\delta_{ref,s} = 0 \quad < \eta^\delta_{ref,s} > \tag{8}$$

$$\tilde{P}^T_{is} = P^{T0}_{is}\left(1 + \lambda_s K^T_i\right) \quad < \eta^{KT}_{is} > \tag{9}$$

$$\tilde{P}^W_{is} = P^{W0}_{is}\left(1 + \lambda_s K^W_i\right) \quad < \eta^{KW}_{is} > \tag{10}$$

$$\tilde{P}^D_{is} = P^{D0}_{is}\left(1 + \lambda_s K^D_i\right) \quad < \eta^{KD}_{is} > \tag{11}$$

Equation (1) shows the objective function that should be maximized. Equation (2) is the power balance at each bus. Equation (3) indicates the power flow through each line. Power generation by each unit is limited by (4)-(5). Thermal limitations of transmission lines are imposed by (6). The voltage angle is restricted by (7). At the reference bus, voltage angle is enforced to be zero by (8). Equations (9)-(11) formulate the increase of generation and load in sending and receiving areas, respectively. Note that $K^T_i = 0, \forall i \in \Omega^{RA}_N$ and $K^D_i = 0, \forall i \in \Omega^{SA}_N$. Dual variables are indicated within $<>$.

As can be seen, the ATC is computed by rising the electric load in the receiving area and the generated power in the sending area until the violation occurs. After solving the linear optimization problem (1)- (11), the optimal λ is used to calculate the ATC as:

$$\begin{aligned} ATC &= \sum\nolimits_{i\in\Omega^{RA}_N} \tilde{P}^D_{is}\left(\lambda^*\right) - \sum\nolimits_{i\in\Omega^{RA}_N} P^{D0}_{is} \\ &= \sum\nolimits_{i\in\Omega^{RA}_N} P^{D0}_{is}\left(1 + \lambda^* K^D_i\right) - \sum\nolimits_{i\in\Omega^{RA}_N} P^{D0}_{is} \end{aligned} \tag{12}$$

B. BI-LEVEL INVESTMENT MODEL FOR TRANSMISSION AND WIND CAPACITY EXPANSION

In this section, a bi-level investment model for joint optimization of transmission and wind capacity expansion is constructed from a centralized perspective. In this regard, the upper level's objective is the total cost minus the weighted ATC. This objective function is subject to the power system's prevailing constraints. The lower level is devoted to calculating the ATC given the solution from the first level. The mathematical bi-level model can be formulated as follows:

$$\underbrace{\text{Maximize}}_{\{P^T_{is},P^L_{ijs},P^W_{is},\overline{P}^W_i,u^L_{ij},\delta_{is}\}} \quad OF^{up}$$

$$= \sum\nolimits_{(ij)} C^L_{ij} u^L_{ij} + \sum\nolimits_i C^W_i \overline{P}^W_i$$

$$+\sum_s N_s \sum_i c_i^T P_{is}^T - \omega \sum_s N_s \lambda_s \tag{13}$$

subject to :

$$P_{is}^T + P_{is}^W - \sum_j P_{ijs}^L = P_{is}^{D0} \tag{14}$$

$$-\left(1-u_{ij}^L\right) M_1 \leq P_{ijs}^L + b_{ij}\left(\delta_{is}-\delta_{js}\right) \leq \left(1-u_{ij}^L\right) M_1 \tag{15}$$

$$0 \leq P_{is}^T \leq \overline{P}_i^T \tag{16}$$

$$0 \leq P_{is}^W \leq \pi_{is} \overline{P}_i^W \tag{17}$$

$$-u_{ij}^L \overline{P}_{ij}^L \leq P_{ijs}^L \leq u_{ij}^L \overline{P}_{ij}^L \tag{18}$$

$$\underline{\delta}_i \leq \delta_{is} \leq \overline{\delta}_i \tag{19}$$

$$\delta_{ref,s} = 0 \tag{20}$$

$$where \lambda_s \in \arg$$

$$\underbrace{Maximize}_{\{\tilde{P}_{is}^T, \tilde{P}_{ijs}^L, \tilde{P}_{is}^W, \tilde{\delta}_{is}, \lambda_s, \tilde{P}_{is}^D\}} \quad OF_s^{lo} = \lambda_s \tag{21}$$

subject to:

$$\text{Constraints } (2)-(11) \tag{22}$$

Equation (13) shows the upper level's objective function. Equation (14) is the power balance at each bus. Equation (15) indicates the power flow through each line. Power generation by thermal and wind farms is bounded by (16)-(17). Lines capacity is denoted by (18). The voltage angle is limited by (19). At the reference bus, the voltage angle is forced to be zero by (20).

It is of note that in the lower-level problem, it is required to know the base generation of thermal units and wind farms. Given the optimal transmission and wind investment expansion plan, the SC-ED must be solved to acquire these values. In this context, the SC-ED is formulated for each scenario as follows:

$$\underbrace{\text{Maximize}}_{\{P_{is}^{T0}, P_{ijs}^{L0}, P_{is}^{W0}, \delta_{js}^0\}} \quad \sum_i c_i^T P_{is}^T \tag{23}$$

subject to :

$$P_{is}^{T0} + P_{is}^{W0} - \sum_j P_{ijs}^{L0} = P_{is}^{D0} \quad < \eta_{is}^{B0} > \tag{24}$$

$$P_{ijs}^{L0} = -u_{ij}^L b_{ij}\left(\delta_{is}^0 - \delta_{js}^0\right) \quad < \eta_{ijs}^{LP0} > \tag{25}$$

$$0 \leq P_{is}^{T0} \leq \overline{P}_i^T \quad < \underline{\eta}_{is}^{T0}, \overline{\eta}_{is}^{T0} > \tag{26}$$

$$0 \leq P_{is}^{W0} \leq \pi_{is} \overline{P}_i^W \quad < \underline{\eta}_{is}^{W0}, \overline{\eta}_{is}^{W0} > \tag{27}$$

$$P_{ijs}^{L0} \leq \overline{P}_{ij}^L \quad < \eta_{ijs}^{L0} > \tag{28}$$

$$\underline{\delta}_i \leq \delta_{is}^0 \leq \overline{\delta}_i \quad < \underline{\eta}_{is}^{\delta 0}, \overline{\eta}_{is}^{\delta 0} > \tag{29}$$

$$\delta_{ref,s} = 0 \quad < \eta_{ref,s}^{\delta 0} > \tag{30}$$

The explanations of these equations have been previously discussed. The equivalent primal-dual formulation for this optimization problem is:

$$\text{Constraints } (24)-(30) \tag{31}$$

$$c_i^T + \eta_{is}^{B0} + \overline{\eta}_{is}^{T0} - \underline{\eta}_{is}^{T0} = 0 \tag{32}$$

$$\eta_{is}^{B0} + \overline{\eta}_{is}^{W0} - \underline{\eta}_{is}^{W0} = 0 \tag{33}$$

$$\overline{\eta}_{is}^{\delta 0} - \underline{\eta}_{is}^{\delta 0} + \sum_j \left\{u_{ij}^L b_{ij}\left(\eta_{ijs}^{LP0} - \eta_{jis}^{LP0}\right)\right\} = 0 \tag{34}$$

$$\eta_{ref,s}^{\delta} + \sum_j \left\{u_{ij}^L b_{ij}\left(\eta_{ijs}^{LP0} - \eta_{jis}^{LP0}\right)\right\} = 0 \tag{35}$$

$$-\eta_{is}^{B0} + \eta_{ijs}^{LP0} + \eta_{ijs}^{L0} = 0 \tag{36}$$

$$\underline{\eta}_{is}^{T0}, \overline{\eta}_{is}^{T0}, \underline{\eta}_{is}^{W0}, \overline{\eta}_{is}^{W0}, \underline{\eta}_{is}^{\delta 0}, \overline{\eta}_{is}^{\delta 0}, \eta_{ijs}^{L0} \geq 0 \tag{37}$$

$$\sum_i c_i^T P_{is}^T = \sum_i \left(-P_{is}^{D0}\eta_{is}^{B0} - \overline{P}_i^T \overline{\eta}_{is}^{T0} - \pi_{is}\overline{P}_i^W \overline{\eta}_{is}^{W0} - \overline{\delta}_i \overline{\eta}_{is}^{\delta 0} + \underline{\delta}_i \underline{\eta}_{is}^{\delta 0}\right) - \sum_{ij} \overline{P}_{ij}^L \eta_{ijs}^{L0} \tag{38}$$

Equation (31) is the primal feasibility constraint of the SC-ED problem. Equations (32)-(37) are the dual feasibility constraints of the SC-ED problem. Equation (38) shows the strong duality. Constraints (31)-(38) are added to the upper-level problem to calculate P_{is}^{T0} and P_{is}^{W0} (the optimal values for the base power flow), which is further used in the lower level to compute the ATC. Notice that adding this set of equations will not change the feasible space of the first level and is solely used to achieve the base values, i.e., optimal generation scheduling.

III. SOLUTION STRATEGY

The primal-dual formulation is employed to solve the presented bi-level structure. In this regard, the second level is substituted by its primal and dual equations and strong duality equality. Hence, the single-level formulation will be as follows:

$$\text{Minimize} \quad OF^{up}$$

$$= \sum_{(ij)} C_{ij}^L u_{ij}^L + \sum_i C_i^W \overline{P}_i^W + \sum_s N_s \sum_i C_i^T P_{is}^T - \omega \sum_s N_s \lambda_s \tag{39}$$

subject to:

$$\text{Equations } (14)-(20) \tag{40}$$

$$\text{Equations } (31)-(38) \tag{41}$$

$$\text{Equations } (2)-(11) \tag{42}$$

$$1 + \sum_i \left(K_i^T P_{is}^{T0} \eta_{is}^{KT} + K_i^D P_{is}^{D0} \eta_{is}^{KD} + K_i^W P_i^{W0} \eta_{is}^{KW}\right) = 0 \tag{43}$$

$$\eta_{is}^B + \eta_{is}^{KT} + \overline{\eta}_{is}^T - \underline{\eta}_{is}^T = 0 \tag{44}$$

$$\eta_{is}^B + \eta_{is}^{KW} + \overline{\eta}_{is}^W - \underline{\eta}_{is}^W = 0 \tag{45}$$

$$\eta_{is}^{KD} - \eta_{is}^B = 0 \tag{46}$$

$$\overline{\eta}_{is}^{\delta} - \underline{\eta}_{is}^{\delta} + \sum_j \left\{u_{ij}^L b_{ij}\left(\eta_{ijs}^{LP} - \eta_{jis}^{LP}\right)\right\} = 0 \tag{47}$$

$$\eta_{ref,s}^{\delta} + \sum_j \left\{u_{ij}^L b_{ij}\left(\eta_{ijs}^{LP} - \eta_{jis}^{LP}\right)\right\} = 0 \tag{48}$$

$$\eta_{ijs}^{LP} + \eta_{ijs}^L - \eta_{is}^B = 0 \tag{49}$$

$$\underline{\eta}_{is}^T, \overline{\eta}_{is}^T, \underline{\eta}_{is}^W, \overline{\eta}_{is}^W, \underline{\eta}_{is}^{\delta}, \overline{\eta}_{is}^{\delta}, \eta_{ijs}^L \geq 0 \tag{50}$$

$$\lambda_s = \sum_i \left(\overline{P}_i^T \overline{\eta}_{is}^T + \pi_{is}\overline{P}_i^W \overline{\eta}_{is}^W + \overline{\delta}_i \overline{\eta}_{is}^\delta - \underline{\delta}_i \underline{\eta}_{is}^\delta + P_{is}^{T0}\eta_{is}^{KT} + P_{is}^{W0}\eta_{is}^{KW} + P_{is}^{D0}\eta_{is}^{KD}\right) + \sum_{ij} \overline{P}_{ij}^L \overline{\eta}_{ijs}^L \quad (51)$$

Due to the existence of bilinear terms $P_{is}^{T0}\eta_{is}^{KT}$, $P_i^{W0}\eta_{is}^{KW}$, $P_{is}^{T0}\lambda_s$, $P_{is}^{W0}\lambda_s$, $\overline{P}_i^W\overline{\eta}_{is}^W$ and $\overline{P}_i^W\overline{\eta}_{is}^{W0}$, the optimization problem formulated above is a bilinear programming model. Although there are some strategies to cope with bilinear terms in optimization problems introducing new binary variables, they may introduce further complexity to the problem. Here, a cutting plane technique named Konno's algorithm is employed [32] to solve the bilinear programming, which will not lead to an increased computational burden. Let us consider two distinct sets of variables as:

$$\begin{aligned}\Omega^{DV} &= \Omega^{DV_1} \cup \Omega^{DV_2} \\ &= \left\{P_{is}^W, \overline{P}_i^W, u_{ij}^L, P_{is}^T, P_{ijs}^L, \delta_{is}, \delta_{ref,s}, P_{is}^{W0}, P_{is}^{T0}, P_{ijs}^{L0}, \delta_{is}^0\right\} \\ &\cup \left\{\begin{array}{l}\lambda_s, \eta_{is}^B, \eta_{ijs}^{LP}, \underline{\eta}_{is}^T, \overline{\eta}_{is}^T, \underline{\eta}_{is}^W, \overline{\eta}_{is}^W, \eta_{ijs}^L, \underline{\eta}_{is}^\delta, \overline{\eta}_{is}^\delta, \eta_{ref,s}^\delta, \\ \eta_{is}^{KT}, \eta_{is}^{KW}, \eta_{is}^{KD} \\ \eta_{is}^{B0}, \eta_{ijs}^{LP0}, \underline{\eta}_{is}^{T0}, \overline{\eta}_{is}^{T0}, \underline{\eta}_{is}^{W0}, \overline{\eta}_{is}^{W0}, \eta_{ijs}^{L0}, \underline{\eta}_{is}^{\delta 0}, \overline{\eta}_{is}^{\delta 0}, \eta_{ref,s}^{\delta 0}\end{array}\right\}\end{aligned}$$

Konno's algorithm is demonstrated in Algorithm 1. First, variables in Ω^{DV_1} are assigned an initial value, which are fixed in the problem rendering in a mixed-integer linear programming (MILP) model. Upon solving this problem, variables in Ω^{DV_2} are obtained. Afterward, the optimal values of Ω^{DV_2} are fixed in the problem, and new values of Ω^{DV_1} are obtained. If the difference in two successive iterations is smaller than a specified tolerance, the algorithm is aborted; otherwise, the algorithm continues.

It is worth mentioning that the product of binary and continuous variables, which appears in (47)-(48), is made linear by the Big-M technique as widely used in the published paper.

Algorithm 1 Konno's Algorithm

Read: Input data and the tolerance ε

Initialization: $k \leftarrow 1$, Set $\Omega^{DV_1} = \Omega^{DV_1^{(k)}}$

Solve bilinear programming for Ω^{DV_2}. Then, set $\Omega^{DV_2} \leftarrow \Omega^{DV_2^{(k)}}$

while $\Omega^{DV_1^{(k+1)}} - \Omega^{DV_1^{(k)}} \leq \varepsilon$ **do**

Solve bilinear programming for Ω^{DV_1} with $\Omega^{DV_2} \leftarrow \Omega^{DV_2^{(k)}}$. Then, set $\Omega^{DV_1^{(k+1)}} \leftarrow \Omega^{DV_1}$, $k \leftarrow k+1$

Solve bilinear programming for Ω^{DV_2} with $\Omega^{DV_1} \leftarrow \Omega^{DV_1^{(k)}}$. Obtain the optimal value of variables in Ω^{DV_2} and set $\Omega^{DV_2} \leftarrow \Omega^{DV_2^{(k)}}$

end while

return optimal variables in $\Omega^{DV} = \Omega^{DV_1} \cup \Omega^{DV_2}$.

IV. SIMULATION STUDIES

This section describes the methodology's successful implementation on the IEEE 24-bus RTS. All solutions are achieved by Gurobi [33] under GAMS [34] using a computer with a 2.5 GHz CPU and 16 GB RAM. The IEEE 24-bus RTS, depicted in Fig. 2, contains 10 power plants (32 units) and 38 lines. As shown in Fig. 2, this grid contains two areas with different voltage levels (138 kV and 230 kV) connected by five tie lines. Candidate lines are represented by red dashed lines. Wind farms' candidate locations are set at buses 15, 16, 18, 19, 20, 21, 22, 23, and 24, where at most 500 MW wind power can be installed. In addition, two existing wind farms are considered at buses 14 and 17. Annualized wind investment cost (C_i^W) is 120 000 \$/MW. The load and generation capacity of thermal units are increased by 70%, and line capacity is decreased by 20% to exert pressure on the transmission grid. Bus 1 is the reference bus. All the data used for experimental results can be downloaded from [35]. Thirty different scenarios model wind-demand uncertainty.

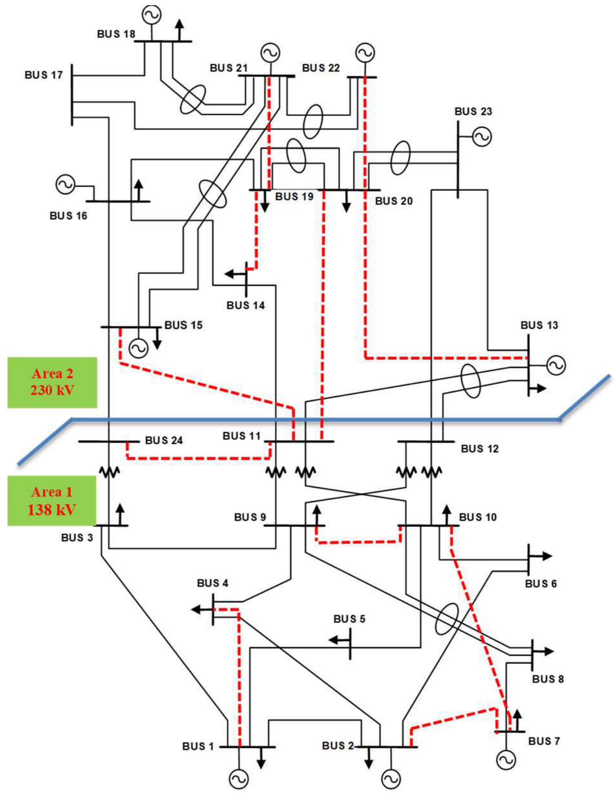

FIGURE 2. IEEE 24-bus RTS.

Table 1 shows the results for two cases: case (a), where planning is conducted without considering ATC, and case (b), where ATC is incorporated into the planning problem. Results provided in Table 1 indicate that it is necessary to construct more transmission lines in case (b), resulting in a higher line investment cost. This higher cost is required to increase the ATC in case (b) compared with case (a). The expected ATC in case (a) is 1176 MW while the expected ATC in case (b) is 1496 MW meaning that ATC increases by 27.2% using the formulated methodology. Notice that the total installed capacity of the wind farm is almost the same in both cases. Moreover, the production cost in case (b) is 4.3% greater than in case (a), which is due to the different network topologies in case (b) with respect to case (a). It is inferred that although

TABLE 1. A comparison of the results for cases (a) and (b) (ω = 3000).

	Case (a): Planning without ATC	Case (b): Planning with ATC
Optimal location (bus number) and capacity (MW) of wind farms	16 (91), 20 (500), 23 (500), 24 (316)	20 (429), 23 (500), 24 (439)
Total wind farm capacity (MW)	1407	1368
Wind investment cost ($)	1.689×10^8	1.642×10^8
Selected candidate lines (From-To)	5 (11-15), 10 (19-21), 11 (20-22)	3 (7-10), 5 (11-15), 6 (11-20), 7 (11-24), 8 (13-20), 10 (19-21), 11 (20-22)
Line investment cost ($)	2.555×10^7	5.951×10^7
Production cost ($)	5.980×10^8	6.241×10^8
Total cost ($)	7.925×10^8	8.479×10^8

the ATC is increased by 27.2% using the presented model, the production cost is also increased by 4.3%.

Fig. 3 depicts the values of ATC for cases (a) and (b) for four distinct scenarios (S_1, S_2, S_3, S_4). In scenarios 1 and 2, the electric demand is minimal, while in scenarios 3 and 4, electric demand is at its highest level. In addition, in scenarios 2 and 3, wind speed is maximum, while in scenarios 1 and 4, wind speed is minimum.

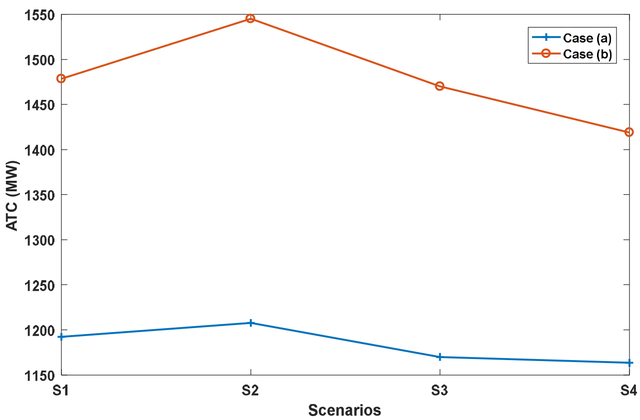

FIGURE 3. ATC values for different scenarios for cases (a) and (b).

As shown in Fig. 3, the values of ATC for the proposed method, i.e., case (b), is larger than the traditional method, i.e., case (a). Furthermore, scenario 2, where the load is minimum and wind generation is maximum, has the highest value of ATC. In contrast, scenario 4, where the load is maximum, and wind generation is minimum, has the lowest value of ATC. These results are already expected because as the load grows, the transmission grid is more congested, leading to a decrease in the ATC. On the other hand, more available wind power at different buses throughout the power system brings more flexibility for producing electric power resulting in a larger ATC.

It would be interesting to investigate the effect of the weighting factor ω on the ATC and the total cost. In this respect, Fig. 4 shows the ATC and total cost versus different values of ω. As shown in Fig. 4, as ω increases, the ATC and total cost also increase. When ω reaches around 8000, no changes in ATC and cost are observed. The highest possible value for ATC is 1942 MW. Increasing the value of ATC above this level is impossible due to the technical limitations of the power grid (here, transmission lines' thermal capacity).

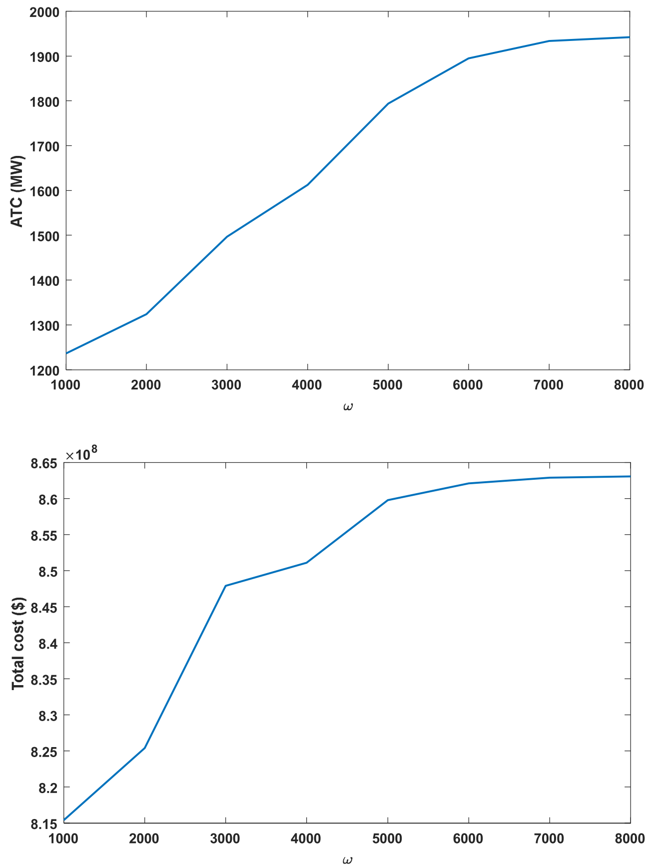

FIGURE 4. ATC and total cost versus ω.

To highlight the importance of ATC, the electric load in area 1 is multiplied by a factor of 60%. Afterward, SC-ED is run for cases (a) and (b). This means the optimal expansion plan (optimal size and locations of wind farms and transmission lines) obtained from case (a) or case (b) is placed and fixed into the power grid. Then, the SC-ED problem is solved for this new power system configuration. It is worth mentioning that under this condition, the load shedding with high penalty cost is added to the objective function to avoid infeasibility. The total amount of load shedding is denoted in Fig. 5 for scenarios S_1, S_2, S_3, and S_4. As shown in Fig. 5, the total load shedding in case (b) is lower than in case (a). This happens because ATC is larger in case (b); hence, more power can be transferred from area 2 to area 1, resulting in less load shedding. Moreover, as expected, load shedding in S_4 has the largest value due to the highest level of load and the lowest level of wind power. Conversely, the load shedding in S_2 has the smallest value due to the lowest level of load and the highest level of wind power.

The total amount of wind curtailment is also denoted in Fig. 6. As can be seen from this plot, wind curtailment in case (b) is less than that in case (a) because in case (b) more

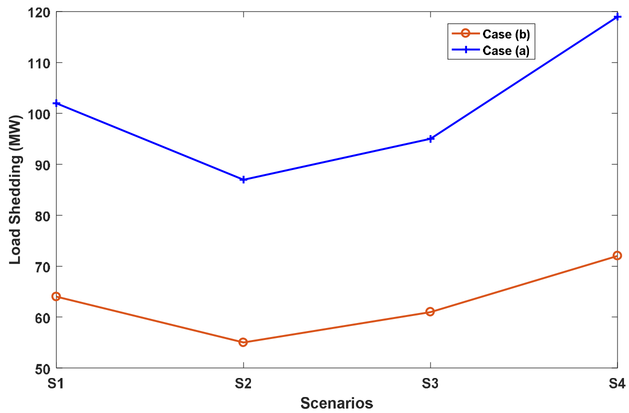

FIGURE 5. **The total amount of load shedding for different scenarios when load increases.**

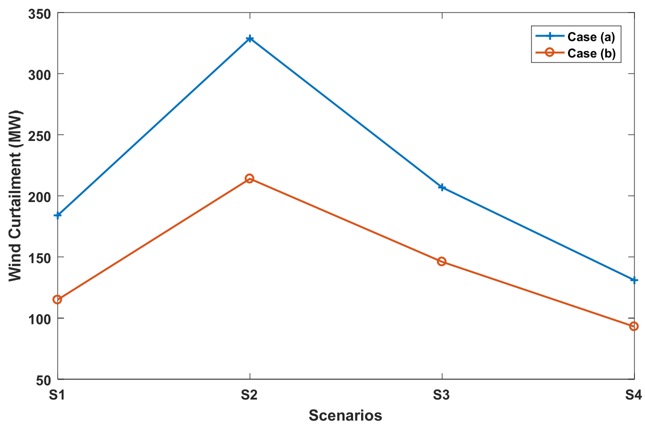

FIGURE 6. **The total amount of wind curtailment for different scenarios when load increases.**

wind power generation can be transferred from area 2 to area 1 due to larger ATC. Additionally, wind curtailment in scenario 2 has the highest value because in this scenario, wind speed is high but the electric demand is minimum. On the contrary, when wind speed is low and load is maximum, the wind curtailment has the smallest value.

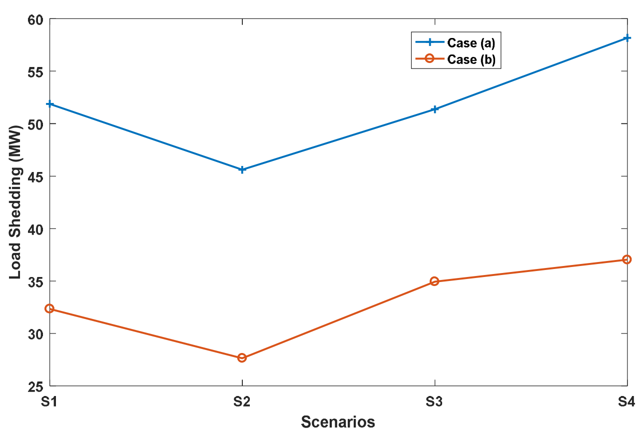

FIGURE 7. **The total amount of load shedding for different scenarios when a generator is shut down.**

To further examine the results, the power plant at bus 7 in area 1 is shut down for the optimal power grid obtained from cases (a) and (b). Then, the SC-ED problem is run for both cases. The results for load shedding are shown in Fig. 7. As can be seen in Fig. 7, the load shedding for case (b) is less than for case (a) because more power can be transferred from area 2 to area 1. Besides, the amount of load shedding varies from one scenario to another due to different electricity demand levels and wind power generation.

The optimal solution is acquired after 15 iterations using Konno's cutting plane algorithm. The convergence curve related to the value of the objective function is plotted in Fig. 8. It takes about 2.107 hours to achieve the optimal solution. It should be highlighted for large-scale power systems the computational burden increases considerably for the proposed model. However, in planning studies an optimal solution of high-quality is more important than solution time. Moreover, decomposition techniques can be employed to help accelerate the entire solution process.

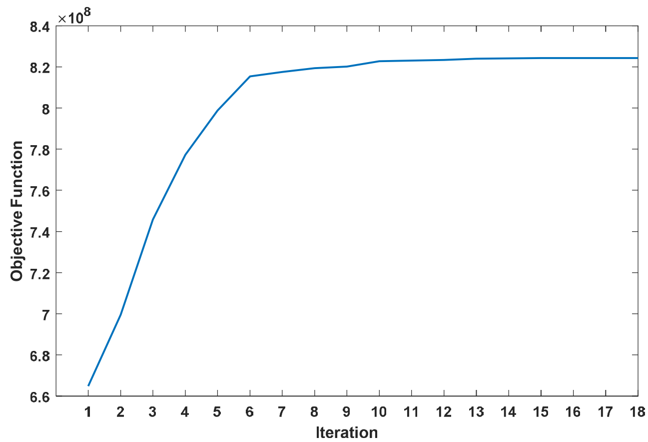

FIGURE 8. **The convergence curve of the objective function's values in different iterations.**

V. CONCLUSION

The ability to enhance the available transfer capability (ATC) of the electricity grid to incorporate a large number of electric power transactions is of utmost importance. To this end, this paper sets out a joint optimization technique for transmission expansion and wind power investment to maximize ATC. The novelty of this work is to present an ATC-based investment model for transmission and wind power expansion that falls into a bi-level structure. The upper level is the investment problem that aims to minimize the total cost while maximizing the ATC. Given the best plan and generation scheduling from the upper level, the lower level calculates the ATC. To solve this problem, the primal-dual formulation is employed where the lower level is replaced by its primal and dual feasibility constraints and strong duality equality. Finally, a single-level bilinear problem emerges, which can be effectively solved by Konno's cutting plane algorithm.

The findings of this work exhibit that the proposed framework can considerably enhance the ATC. The main conclusions of this study are listed as follows:

1) The presented model can effectively increase the ATC value at the expense of more cost. This enhanced ATC improves system security and promotes competition among market participants.
2) In the case of a contingency or load growth, the amount of load shedding in the proposed model is less than that in the conventional models because more power can be transferred using the proposed method.
3) Amount of wind curtailment in the proposed method is smaller than that in the traditional method since more generated wind power can be transferred from one area to another leading to a reduction in wind power curtailment.

The extension of this work to include AC power flow for ATC evaluation is proposed as future work. In addition, since FACTS devices can entirely change the power flow, it is needed to model such technologies in the planning studies and ATC assessment problem. Stationary and mobile ESSs can also be employed to examine their effects on the ATC.

ACKNOWLEDGMENT

The authors extend their appreciation to the Deputyship for Research & Innovation, Ministry of Education in Saudi Arabia for funding this research work through the project no. (IFKSURG-2-1322).

REFERENCES

[1] H. Zhang, H. Cheng, L. Liu, S. Zhang, Q. Zhou, and L. Jiang, "Coordination of generation, transmission and reactive power sources expansion planning with high penetration of wind power," *Int. J. Elect. Power Energy Syst.*, vol. 108, pp. 191–203, Jun. 2019.

[2] D. Liu, S. Zhang, H. Cheng, L. Liu, J. Zhang, and X. Zhang, "Reducing wind power curtailment by risk-based transmission expansion planning," *Int. J. Electr. Power Energy Syst.*, vol. 124, Jan. 2021, Art. no. 106349.

[3] C. A. Moraes, L. W. de Oliveira, E. J. de Oliveira, D. F. Botelho, A. N. de Paula, and M. F. Pinto, "A probabilistic approach to assess the impact of wind power generation in transmission network expansion planning," *Electr. Eng.*, vol. 104, no. 2, pp. 1029–1040, Apr. 2022.

[4] M. Sun, J. Cremer, and G. Strbac, "A novel data-driven scenario generation framework for transmission expansion planning with high renewable energy penetration," *Appl. Energy*, vol. 228, pp. 546–555, Oct. 2018.

[5] G. Pulazza, N. Zhang, C. Kang, and C. A. Nucci, "Transmission planning with battery-based energy storage transportation for power systems with high penetration of renewable energy," *IEEE Trans. Power Syst.*, vol. 36, no. 6, pp. 4928–4940, Nov. 2021.

[6] M. Jadidoleslam, A. Ebrahimi, and M. A. Latify, "Probabilistic transmission expansion planning to maximize the integration of wind power," *Renew. Energy*, vol. 114, pp. 866–878, Dec. 2017.

[7] S. Zolfaghari and T. Akbari, "Bilevel transmission expansion planning using second-order cone programming considering wind investment," *Energy*, vol. 154, pp. 455–465, Jul. 2018.

[8] M. Kazemi and M. R. Ansari, "An integrated transmission expansion planning and battery storage systems placement—A security and reliability perspective," *Int. J. Electr. Power Energy Syst.*, vol. 134, Jan. 2022, Art. no. 107329.

[9] A. Moreira, D. Pozo, A. Street, and E. Sauma, "Reliable renewable generation and transmission expansion planning: Co-optimizing system's resources for meeting renewable targets," *IEEE Trans. Power Syst.*, vol. 32, no. 4, pp. 3246–3257, Jul. 2017.

[10] L. Baringo and A. J. Conejo, "Transmission and wind power investment," *IEEE Trans. Power Syst.*, vol. 27, no. 2, pp. 885–893, May 2012.

[11] A. Arabali, M. Ghofrani, M. Etezadi-Amoli, M. S. Fadali, and M. Moeini-Aghtaie, "A multi-objective transmission expansion planning framework in deregulated power systems with wind generation," *IEEE Trans. Power Syst.*, vol. 29, no. 6, pp. 3003–3011, Nov. 2014.

[12] S. L. Gbadamosi, N. I. Nwulu, and Y. Sun, "Multi-objective optimisation for composite generation and transmission expansion planning considering offshore wind power and feed-in tariffs," *IET Renew. Power Gener.*, vol. 12, no. 14, pp. 1687–1697, Oct. 2018.

[13] X. Wang, Z. Bie, F. Liu, Y. Kou, and L. Jiang, "Bi-level planning for integrated electricity and natural gas systems with wind power and natural gas storage," *Int. J. Electr. Power Energy Syst.*, vol. 118, Jun. 2020, Art. no. 105738.

[14] Y. Wang, S. Lou, Y. Wu, M. Lv, and S. Wang, "Coordinated planning of transmission expansion and coal-fired power plants flexibility retrofits to accommodate the high penetration of wind power," *IET Gener., Transmiss. Distrib.*, vol. 13, no. 20, pp. 4702–4711, Oct. 2019.

[15] G. A. Orfanos, P. S. Georgilakis, and N. D. Hatziargyriou, "Transmission expansion planning of systems with increasing wind power integration," *IEEE Trans. Power Syst.*, vol. 28, no. 2, pp. 1355–1362, May 2013.

[16] N. Yang, T. Qin, L. Wu, Y. Huang, Y. Huang, C. Xing, L. Zhang, and B. Zhu, "A multi-agent game based joint planning approach for electricity-gas integrated energy systems considering wind power uncertainty," *Electr. Power Syst. Res.*, vol. 204, Mar. 2022, Art. no. 107673.

[17] E. Mortaz and J. Valenzuela, "Evaluating the impact of renewable generation on transmission expansion planning," *Electr. Power Syst. Res.*, vol. 169, pp. 35–44, Apr. 2019.

[18] F. Ugranli and E. Karatepe, "Transmission expansion planning for wind turbine integrated power systems considering contingency," *IEEE Trans. Power Syst.*, vol. 31, no. 2, pp. 1476–1485, Mar. 2016.

[19] F. Ugranlı and E. Karatepe, "Multi-objective transmission expansion planning considering minimization of curtailed wind energy," *Int. J. Electr. Power Energy Syst.*, vol. 65, pp. 348–356, Feb. 2015.

[20] E. Naderi, M. Pourakbari-Kasmaei, and M. Lehtonen, "Transmission expansion planning integrated with wind farms: A review, comparative study, and a novel profound search approach," *Int. J. Electr. Power Energy Syst.*, vol. 115, Feb. 2020, Art. no. 105460.

[21] Z. Zhuo, E. Du, N. Zhang, C. Kang, Q. Xia, and Z. Wang, "Incorporating massive scenarios in transmission expansion planning with high renewable energy penetration," *IEEE Trans. Power Syst.*, vol. 35, no. 2, pp. 1061–1074, Mar. 2020.

[22] S. Abbasi and H. Abdi, "Multiobjective transmission expansion planning problem based on ACOPF considering load and wind power generation uncertainties," *Int. Trans. Electr. Energy Syst.*, vol. 27, no. 6, Jun. 2017, Art. no. e2312.

[23] Z. Wu, Y. Liu, W. Gu, Y. Wang, and C. Chen, "Contingency-constrained robust transmission expansion planning under uncertainty," *Int. J. Electr. Power Energy Syst.*, vol. 101, pp. 331–338, Oct. 2018.

[24] D. Xiao and H. Chen, "Stochastic up to congestion bidding strategy in the nodal electricity markets considering risk management," *IEEE Access*, vol. 8, pp. 202428–202438, 2020.

[25] A. Almalaq, K. Alqunun, M. M. Refaat, A. Farah, F. Benabdallah, Z. M. Ali, and S. H. E. A. Aleem, "Towards increasing hosting capacity of modern power systems through generation and transmission expansion planning," *Sustainability*, vol. 14, no. 5, p. 2998, Mar. 2022.

[26] B. Chen, T. Liu, X. Liu, C. He, L. Nan, L. Wu, and X. Su, "Distributionally robust coordinated expansion planning for generation, transmission, and demand side resources considering the benefits of concentrating solar power plants," *IEEE Trans. Power Syst.*, vol. 38, no. 2, pp. 1205–1218, Mar. 2023.

[27] M. A. El-Meligy, A. M. El-Sherbeeny, A. T. A. Soliman, A. E. E. A. Elgawad, and E. A. Naser, "On the solution of robust transmission expansion planning using duality theorem under polyhedral uncertainty set," *Electric Power Syst. Res.*, vol. 206, May 2022, Art. no. 107785.

[28] C. Li, A. J. Conejo, P. Liu, B. P. Omell, J. D. Siirola, and I. E. Grossmann, "Mixed-integer linear programming models and algorithms for generation and transmission expansion planning of power systems," *Eur. J. Oper. Res.*, vol. 297, no. 3, pp. 1071–1082, Mar. 2022.

[29] Z. Luburic, H. Pandzic, and M. Carrion, "Transmission expansion planning model considering battery energy storage, TCSC and lines using AC OPF," *IEEE Access*, vol. 8, pp. 203429–203439, 2020.

[30] Y. Ou and C. Singh, "Assessment of available transfer capability and margins," *IEEE Power Eng. Rev.*, vol. 22, no. 5, p. 69, May 2002.

[31] T. Akbari, A. Rahimikian, and A. Kazemi, "A multi-stage stochastic transmission expansion planning method," *Energy Convers. Manage.*, vol. 52, nos. 8–9, pp. 2844–2853, Aug. 2011.

[32] H. Konno, "A cutting plane algorithm for solving bilinear programs," *Math. Program.*, vol. 11, no. 1, pp. 14–27, 1976.
[33] Gurobi Optimization. *Gurobi Optimizer Reference Manual*. [Online]. Available: http://www.gurobi.com
[34] G. U. Guide, *GAMS Development Corporation*. Washington, DC, USA, 2014.
[35] M. A. Elmeligy *Data for: Transmission Expansion Planning Considering a High Share of Wind Power to Maximize Available Transfer Capability*. [Online]. Available: https://drive.google.com/file/d/1wSp8EVUv04Xsb-LochdfFjpmWjT4qjZz/view?usp=share_link

AHMAD M. ALSHAMRANI received the Ph.D. degree in operations research from Case Western Reserve University, USA. He is currently an Associate Professor with the Department of Statistics and Operations Research, King Saud University, where he served as the Department Head for eight years. He has done administrative and consultations work for many organizations. His research interests include mathematical programming, inventory, and optimization in general.

MOHAMMED A. EL-MELIGY received the B.Sc. degree in information technology from Menoufia University, Egypt, in 2005. He has been a Software Engineer with King Saud University, Riyadh, Saudi Arabia, since 2009. His research interests include petri nets, supervisory control of discrete event systems, database software, and network administration.

MOHAMED ABDEL FATTAH SHARAF received the Ph.D. degree in industrial engineering from Chiba University, Japan. He is currently the Head of the Development and Quality Unit, College of Engineering, King Saud University. He has published more than 30 articles in the areas of spare parts control, quality management, maintenance, six-sigma methodology, and academic accreditation.

WIGDAN AREF MOHAMMED SAIF is currently pursuing the Ph.D. degree with the Industrial Engineering Department, King Saud University. He was a Teaching Assistant with the Industrial Engineering Department.

EMAD MAHROUS AWWAD is currently pursuing the Ph.D. degree with the Electrical Engineering Department, King Saud University. He was a Teaching Assistant with the Industrial Electronics and Control Engineering Department, Faculty of Electronic Engineering, Menofia University, Egypt. He has developed his research studies in the field of design, control, and implementation of autonomous mobile robot. He is interested in modeling, optimization, observer design, and MPC controller of vehicle dynamics, under the wheel–terrain interaction slippage phenomenon. He is also interested in artificial intelligence, machine learning, and deep learning, related to the field of robotics and image processing.